

Supporting Information

Enabling high-performance and high-rate-capability $\text{Na}_4\text{MnV}(\text{PO}_4)_3$ sodium-ion battery cathodes through tuning the NASICON framework

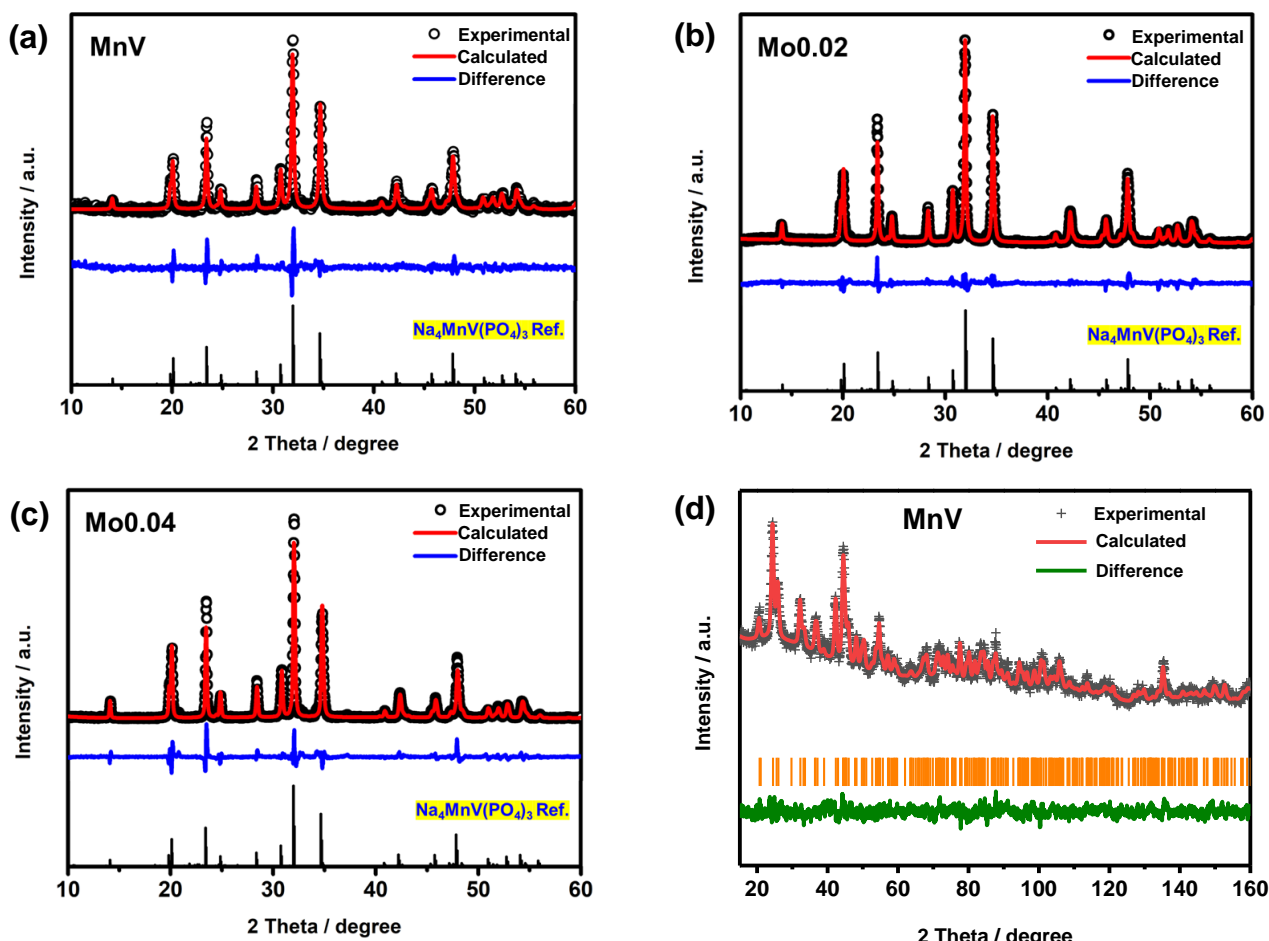


Figure S1. Rietveld refinement profiles using XRD data of the NASICON-type structure Mo-doped $\text{Na}_4\text{MnV}(\text{PO}_4)_3$ (precursor molar ratio of Mo to NMVP = 0, 0.02, 0.03, 0.04, denoted as MnV, Mo0.02, Mo0.03, and Mo0.04, respectively) cathode material for compositions (a) MnV, (b) Mo0.02, and (c) Mo0.04. (d) The refined fit profile against neutron powder diffraction pattern of MnV powder ($\text{R}_{\text{wp}} = 3.43\%$, GOF: 1.42)

Table S1. Refined structure of Na₄MnV(PO₄)₃ using XRD

Space group = $R\bar{3}c$	$a = b = 8.965(7) \text{ \AA}, c = 21.574(2) \text{ \AA},$ Volume = 1501.885(5) \AA^3			
$R_{wp} = 4.75\%, R_{exp} = 8.24\%, R_p = 6.13\%, GOF: 1.73$				
Atom	Mult.	x	y	z
Na1	6	0.00000	0.00000	0.00000
Na2	18	0.64250	0.00000	0.25000
O1	36	0.01360	0.20900	0.19320
O2	36	0.18360	0.17210	0.08520
Mn	12	0.00000	0.00000	0.14901
V	12	0.00000	0.00000	0.14901
P	18	0.29800	0.00000	0.25000

Footnotes: R_{wp} : R-weighted pattern; R_{exp} : R-expected; R_p : R-pattern; GOF: goodness-of-fit

Table S2. Refined structure of Mo0.02 using XRD

Space group = $R\bar{3}c$	$a = b = 8.968(6) \text{ \AA}, c = 21.540(8) \text{ \AA},$ Volume = 1500.521(4) \AA^3			
$R_{wp} = 7.51\%, R_{exp} = 13.35\%, R_p = 10.20\%, GOF: 1.78$				
Atom	Mult.	x	y	z
Na1	6	0.00000	0.00000	0.00000
Na2	18	0.64250	0.00000	0.25000
O1	36	0.01360	0.20900	0.19320
O2	36	0.18360	0.17210	0.08520
Mn	12	0.00000	0.00000	0.14901
V	12	0.00000	0.00000	0.14901
P	18	0.29800	0.00000	0.25000
Mo	12	0.29800	0.00000	0.25000

Table S3. Refined structure of Mo0.03 using XRD

Space group = $R\bar{3}c$	$a = b = 8.963(4) \text{ \AA}, c = 21.479(2) \text{ \AA},$ $\text{Volume} = 1494.552(8) \text{ \AA}^3$			
$R_{wp} = 7.95\%, R_{exp} = 13.54\%, R_p = 10.08\%, \text{GOF: } 1.70$				
Atom	Mult.	x	y	z
Na1	6	0.00000	0.00000	0.00000
Na2	18	0.64250	0.00000	0.25000
O1	36	0.01360	0.20900	0.19320
O2	36	0.18360	0.17210	0.08520
Mn	12	0.00000	0.00000	0.14901
V	12	0.00000	0.00000	0.14901
P	18	0.29800	0.00000	0.25000
Mo	12	0.29800	0.00000	0.25000

Table S4. Refined structure of Mo0.04 using XRD

Space group = $R\bar{3}c$	$a = b = 8.935(3) \text{ \AA}, c = 21.485(9) \text{ \AA},$ $\text{Volume} = 1484.630(7) \text{ \AA}^3$			
$R_{wp} = 6.95\%, R_{exp} = 16.36\%, R_p = 12.68\%, \text{GOF: } 1.80$				
Atom	Mult.	x	y	z
Na1	6	0.00000	0.00000	0.00000
Na2	18	0.64250	0.00000	0.25000
O1	36	0.01360	0.20900	0.19320
O2	36	0.18360	0.17210	0.08520
Mn	12	0.00000	0.00000	0.14901
V	12	0.00000	0.00000	0.14901
P	18	0.29800	0.00000	0.25000
Mo	12	0.29800	0.00000	0.25000

Table S5. The detailed crystallography of MnV cathode obtained through joint refinement against NPD and XRD data.

Space group = $R\bar{3}c$			$a = b = 8.953(8) \text{ \AA}$, $c = 21.484(9) \text{ \AA}$, Volume $1491.7(5) \text{ \AA}^3$			
$R_{wp} = 3.43\%$, GOF: 1.42						
Atom	Mult.	x	y	z	Occupancy	UISO
Na1	6	0.00000	0.00000	0.00000	1	0.044(5)
Na2	18	0.6427(1)	0.00000	0.25000	1	0.063(4)
O1	36	0.0108(7)	0.2056(7)	0.1921(8)	1	0.035(8)
O2	36	0.1875(5)	0.1724(5)	0.0856(5)	1	0.019(4)
Mn	12	0.00000	0.00000	0.1489(3)	0.5	0.029(1)
V	12	0.00000	0.00000	0.1489(3)	0.5	0.029(1)
P	18	0.2987(5)	0.00000	0.25000	1	0.011(7)

Table S6. The detailed crystallography of Mo0.03 cathode obtained through joint refinement against NPD and XRD data.

Space group = $R\bar{3}c$			$a = b = 8.953(4) \text{ \AA}$ $c = 21.456(8) \text{ \AA}$, Volume = $1489.6(1) \text{ \AA}^3$			
$R_{wp} = 4.32\%$, GOF: 1.65						
Atom	Mult.	x	y	z	Occupancy	UISO
Na1	6	0.00000	0.00000	0.00000	1	0.038(3)
Na2	18	0.6396(7)	0.00000	0.25000	1	0.050(2)
O1	36	0.0131(4)	0.2083(4)	0.1921(1)	1	0.035(1)
O2	36	0.1864(3)	0.1716(3)	0.0848(1)	1	0.022(1)
Mn	12	0.00000	0.00000	0.1492(1)	0.5	0.016(2)
V	12	0.00000	0.00000	0.1492(1)	0.5	0.016(2)
P	18	0.2988(3)	0.00000	0.25000	0.97	0.014(1)
Mo	18	0.2988(3)	0.00000	0.25000	0.03	0.014(1)

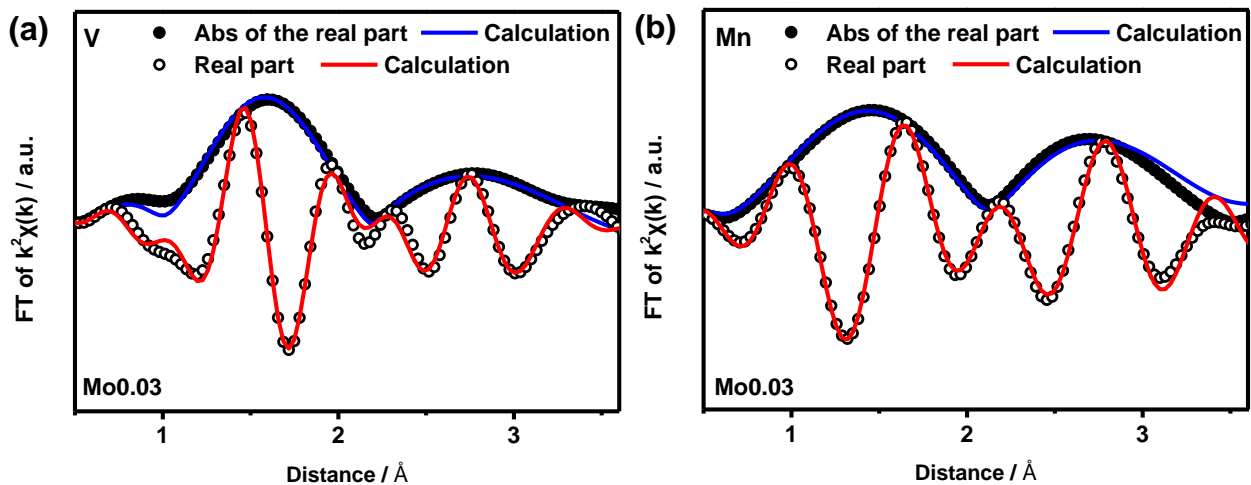


Figure S2. EXAFS spectrum of Mo0.03 at the (a) V and (b) Mn K -edge with model fits

Table S7. EXAFS model analysis results

Element	Shell	Coordination Number	$r / \text{\AA}$	$\sigma^2 \times 10^{-3} / \text{\AA}^2$	$\Delta E / \text{eV}$	R
Mn	Mn–O	6	2.15(7)	0.0031(8)	3.311	0.0069(9)
	Mn–P	4	3.57(9)	0.0053(1)		
V	V–O	6	2.06(2)	0.0027(6)	5.635	0.0158(1)
	V–P	4	3.61(1)	0.0072(6)		

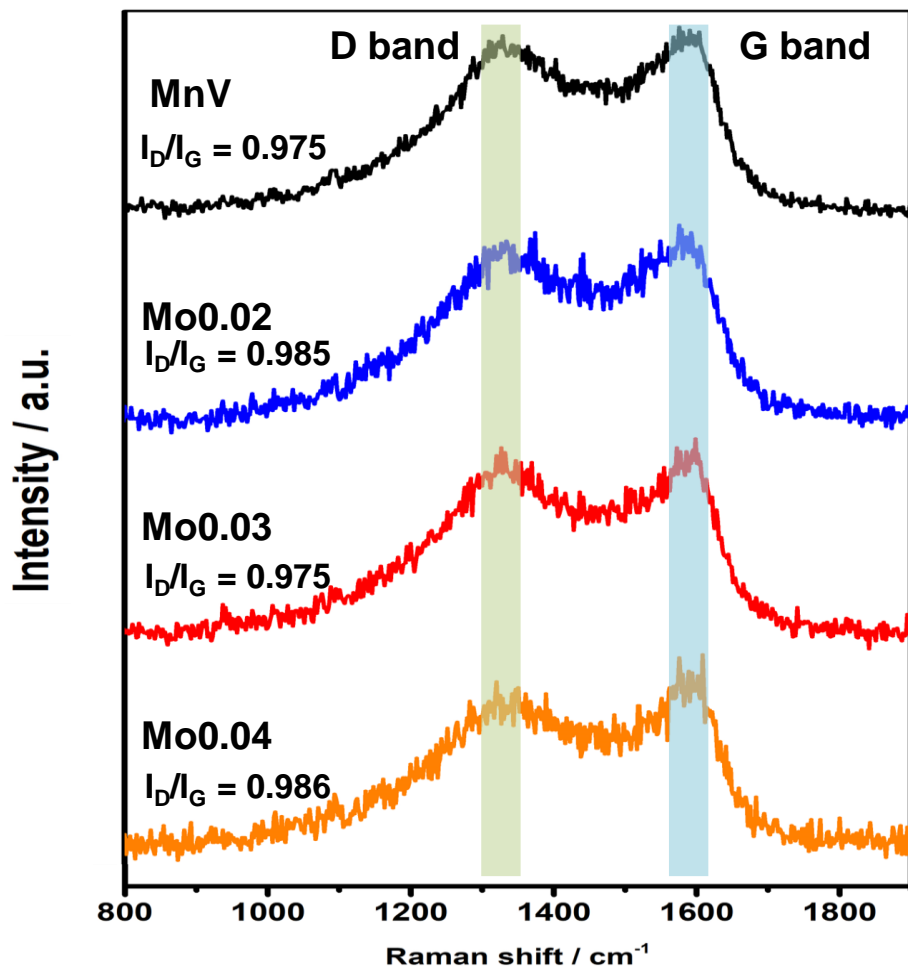


Figure S3. Raman spectrum of MnV, Mo0.02, Mo0.03, and Mo0.04 cathodes. Data are offset in y for clarity. D and G bands are shaded in green and blue, respectively.

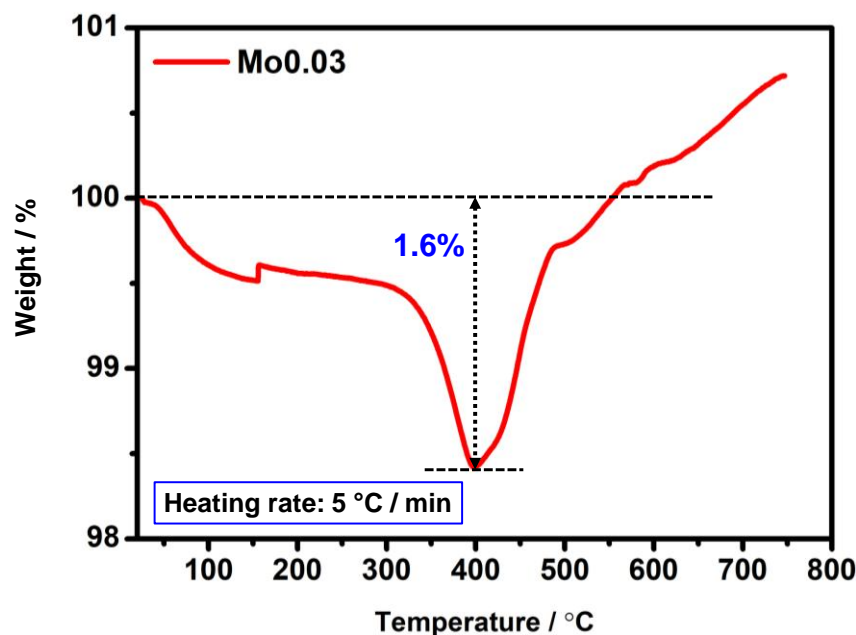


Figure S4. Thermogravimetry analysis (TGA) data for Mo0.03

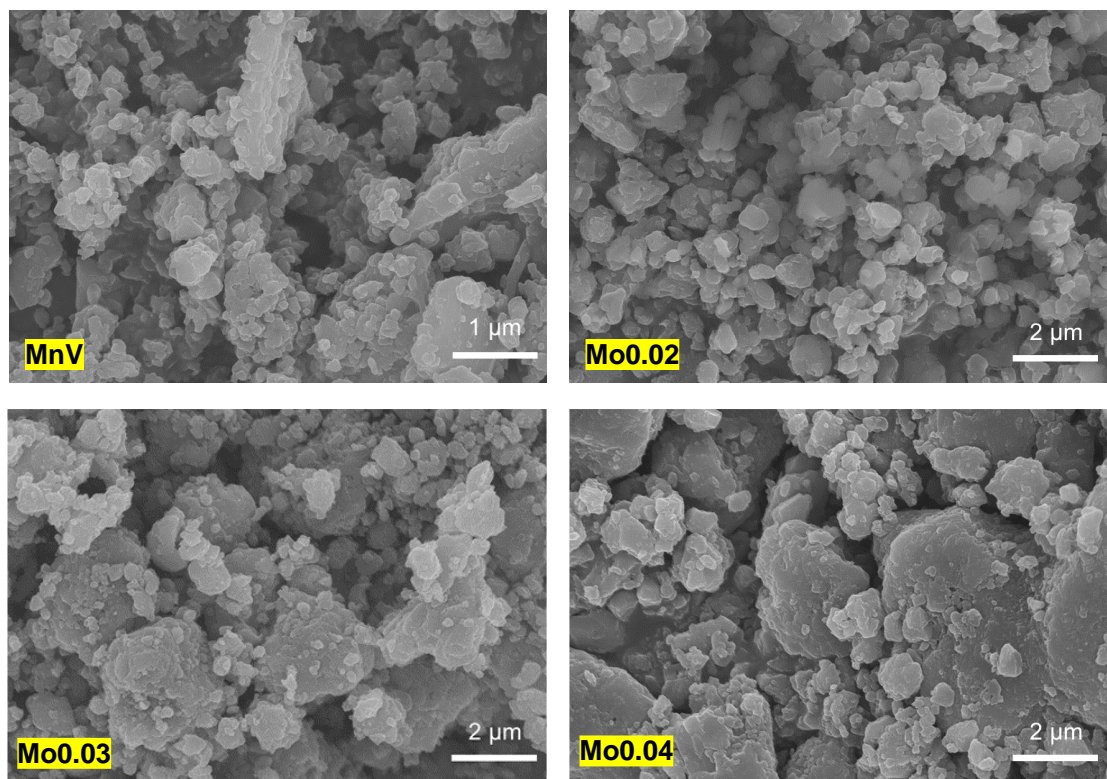


Figure S5. Typical SEM images of MnV, Mo0.02, Mo0.03, and Mo0.04 cathodes

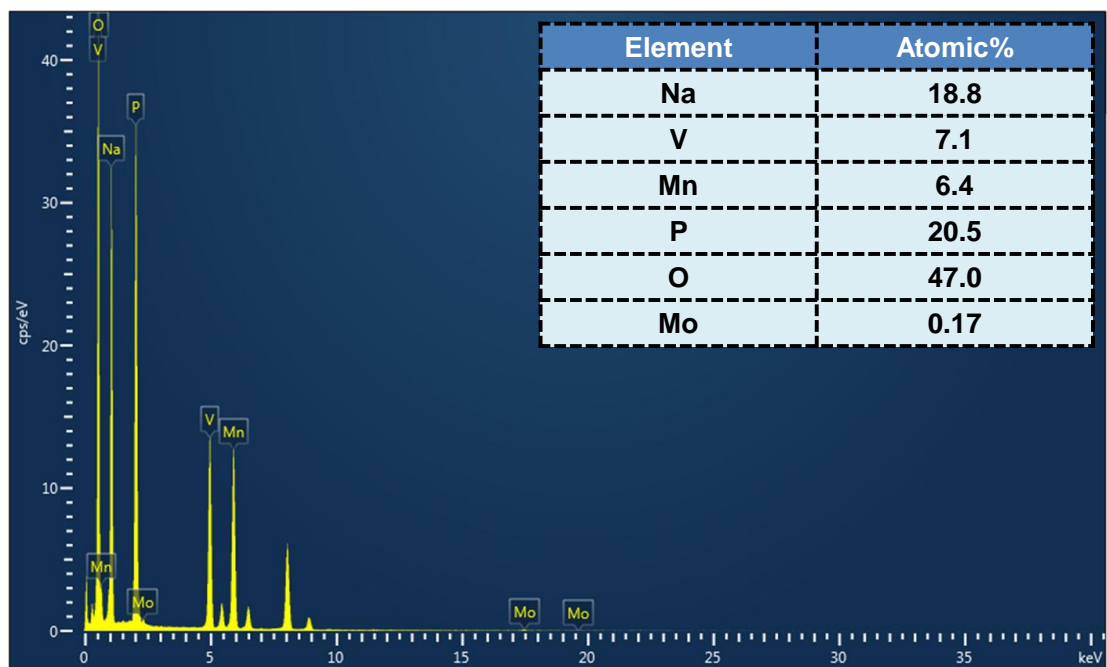


Figure S6. EDS results and derived elemental composition of the Mo0.03 cathode

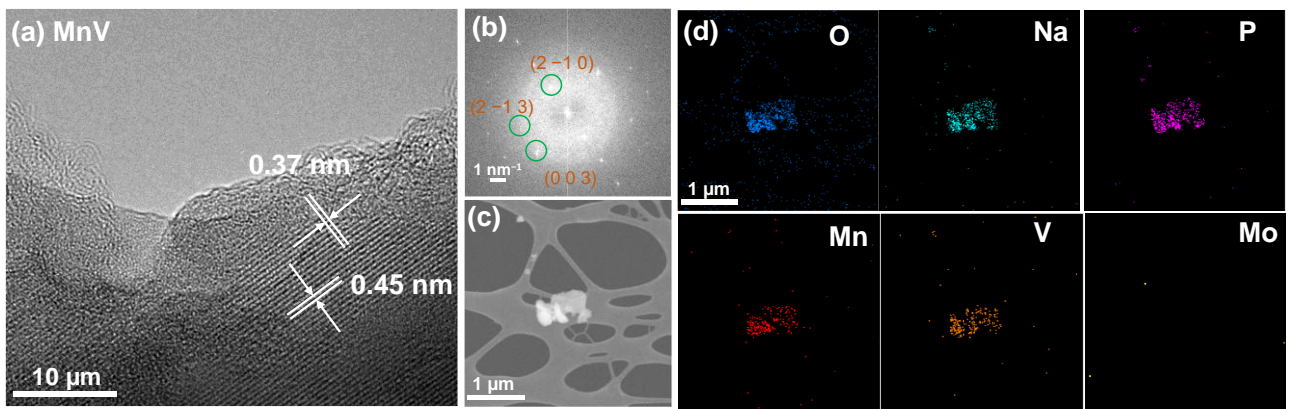


Figure S7. Typical (a) TEM image with corresponding (b) fast Fourier transform, (d) TEM image with corresponding (e) elemental mapping using EDS, of MnV.

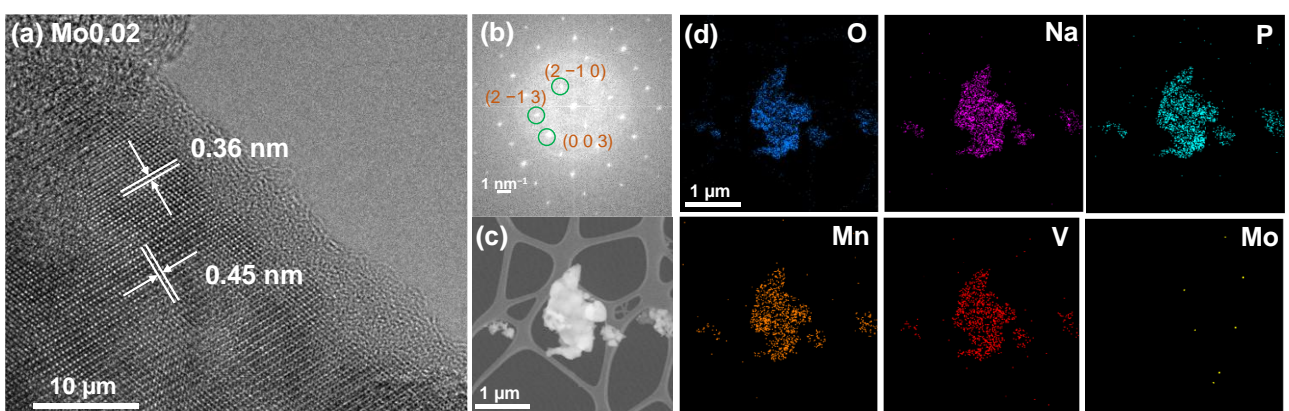


Figure S8. Typical (a) TEM image with corresponding (b) fast Fourier transform, (d) TEM image with corresponding (e) elemental mapping using EDS, of Mo0.02.

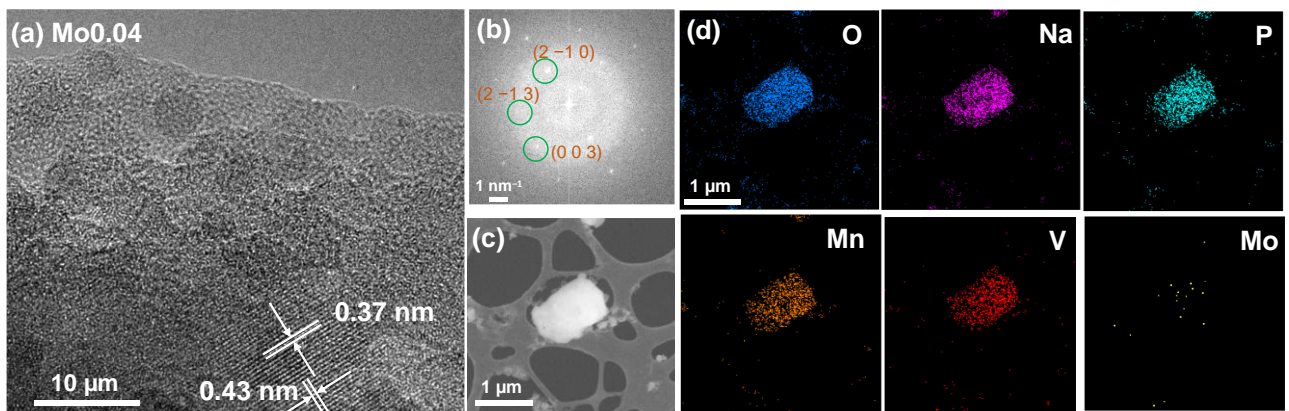
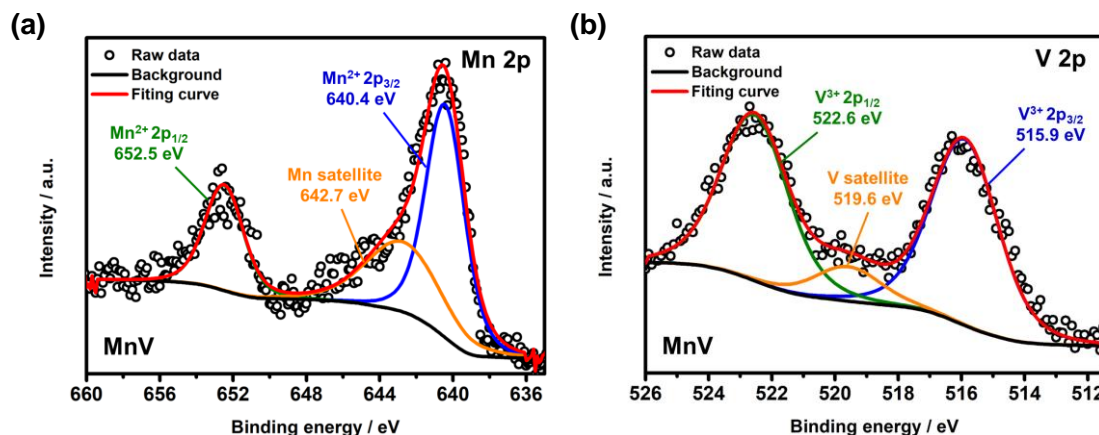


Figure S9. Typical (a) TEM image with corresponding (b) fast Fourier transform, (d) TEM image with corresponding (e) elemental mapping using EDS, of Mo0.04.

Table S8. ICP-MS determined elemental composition of MnV, Mo0.02, Mo0.03, and Mo0.04 cathodes

Samples	Na	V	Mn	P	Mo
MnV	4.1742	1.2198	1.0656	3.5404	0
Mo0.02	4.2519	1.1620	1.0183	3.5489	0.019
Mo0.03	4.1917	1.1477	1.0790	3.5504	0.0313
Mo0.04	4.1819	1.1589	1.0591	3.5543	0.0458

**Figure S10.** (a) Mn and (b) V 2p XPS data of MnV with fitting.**Table S9.** Calculated and experimental lattice constants of Na₄MnV(PO₄)₃.

	a (Å)	b (Å)	c (Å)	Volume (Å ³)
This work (cal.)	8.9471	8.9471	21.4567	1487.6
Gao, <i>et al.</i> (2020) [1]	8.9398	8.9398	21.5317	1490.26
This work (exp.)	8.9540	8.9540	21.4850	1491.7

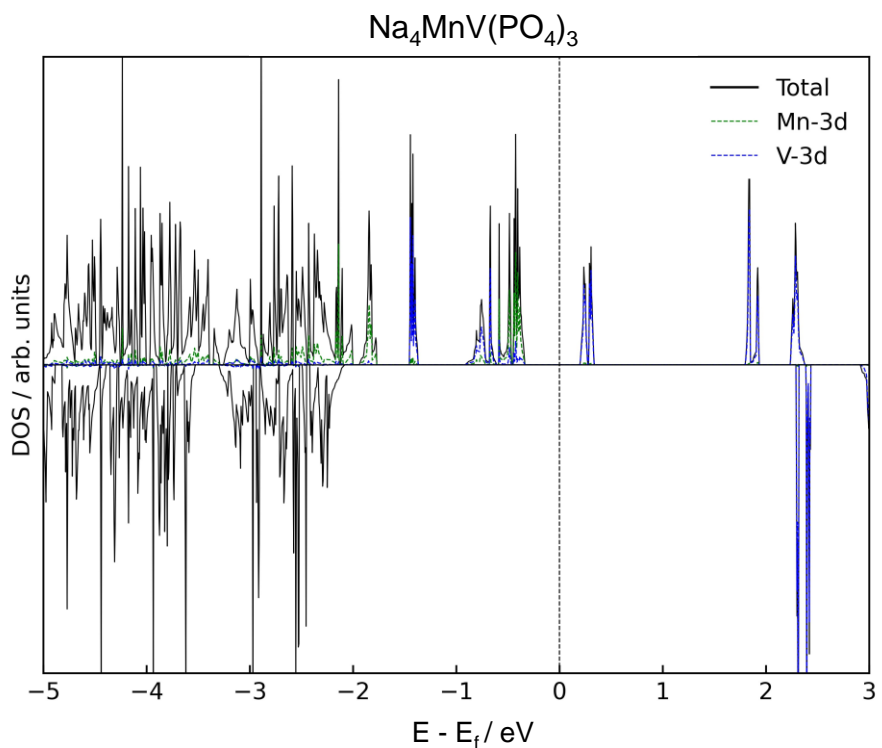


Figure S11. The calculated total and partial DOS of $\text{Na}_4\text{MnV}(\text{PO}_4)_3$. The Fermi level is set to zero as displayed by the dashed line.

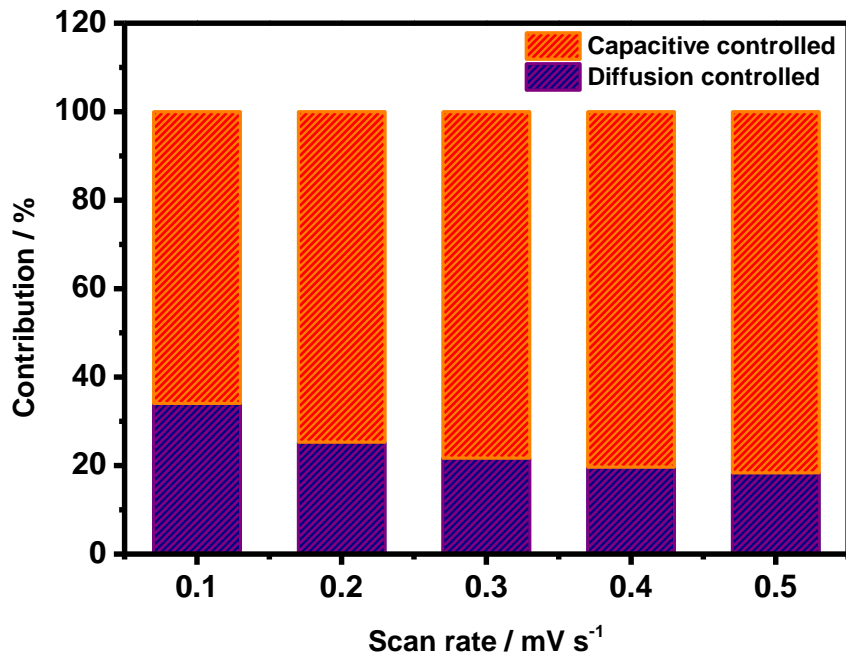


Figure S12. The capacitive (orange) and diffusion (purple) contribution to capacity at different scan rates from 0.1 to 0.5 mV s^{-1} of Mo0.03.

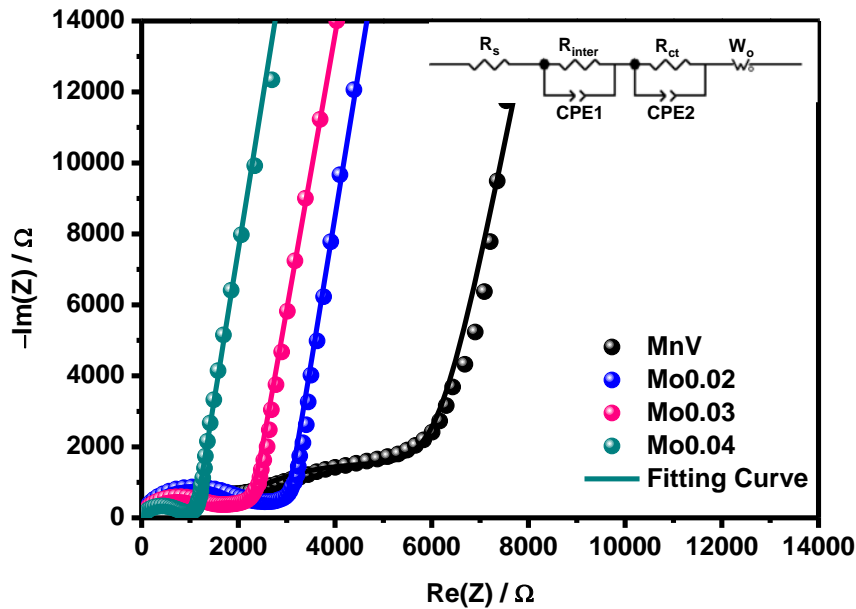


Figure S13. Electrochemical Impedance Spectroscopy (EIS) of MnV, Mo0.02, Mo0.03, and Mo0.04.

Table S10. Comparison of battery performance with other similar works in the literature.

Cathode	Specific capacity / mAh g ⁻¹	Rate retention / mAh g ⁻¹	Cycling stability	Ref.
Mo-doped Na ₄ MnV(PO ₄) ₃ /C	97.5 at 0.2C	85.4 at 1C 69.2 at 5C 46.4 at 20C	78.8% at 1C, 300 cycles	Our work
Na ₄ VMn _{0.75} Mg _{0.25} (PO ₄) ₃	79 at 0.1C	80 at 5C	70% at 1C, 100 cycles	[2]
Na _{3.75} VMn _{0.75} Al _{0.25} (PO ₄) ₃	93 at 0.1C	82 at 5C	96% at 1C, 100 cycles	[2]
Na _{3.9} Mn _{0.95} Zr _{0.05} V(PO ₄) ₃ /C	108.8 at 0.2C	97 at 10C 88 at 20C	81.2% at 1C, 500 cycles	[3]
Na ₄ VMn _{0.9} Cu _{0.1} (PO ₄) ₃ /C	117 at 0.25C	68 at 40C	86% at 30C, 3000 cycles	[4]

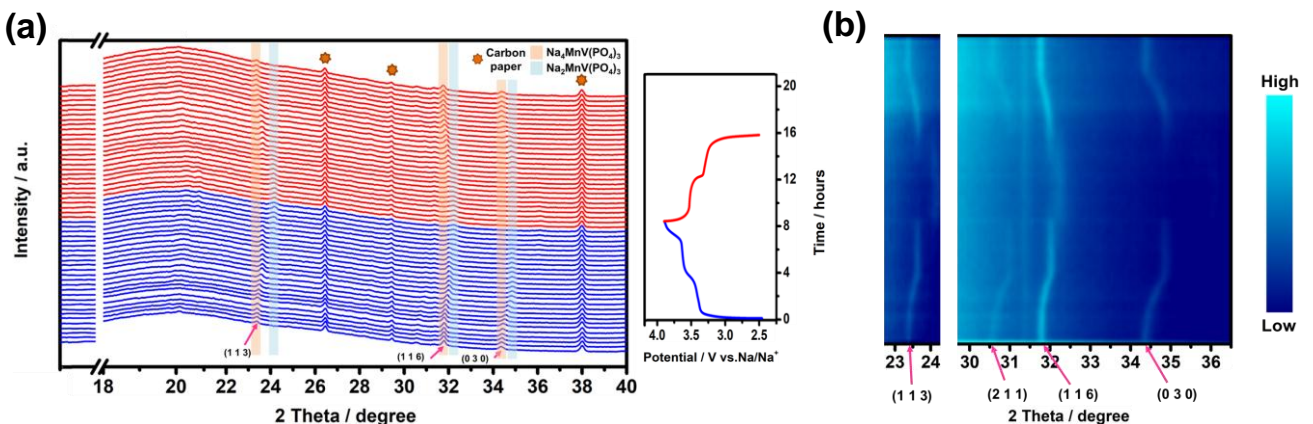


Figure S14. *In operando* XRD data of the MnV electrode shown as (a) 1 dimensional diffraction data offset in y for clarity and (b) as a contour map with intensity in colour as per the legend shown right.

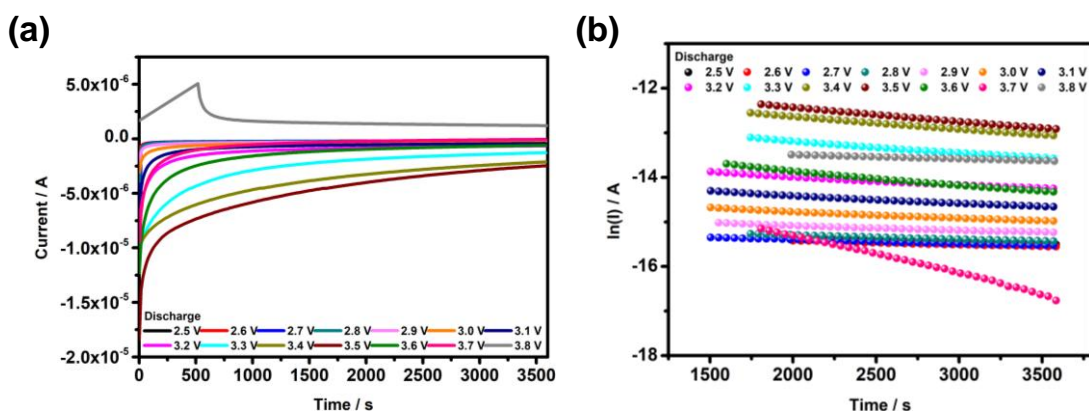


Figure S15. (a) First cycle discharge I–t and (b) $\ln(I)$ –t plots of the MnV electrode.

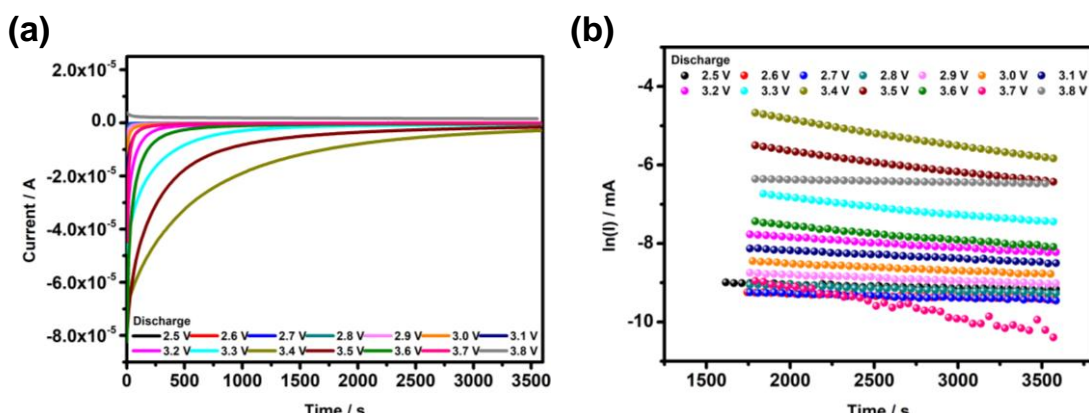


Figure S16. (a) First cycle discharge I–t and (b) $\ln(I)$ –t plots of the Mo_{0.03} electrode.

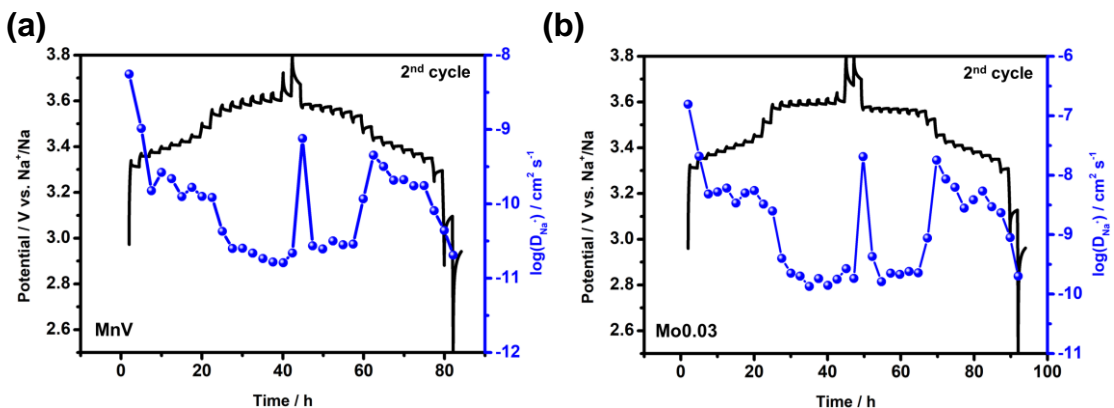


Figure S17. Second cycle GITT charge/discharge and calculated $\log(D_{Na^+})$ plots for (a) MnV; (b) Mo0.03. Lines through the points are a guide to the eye.

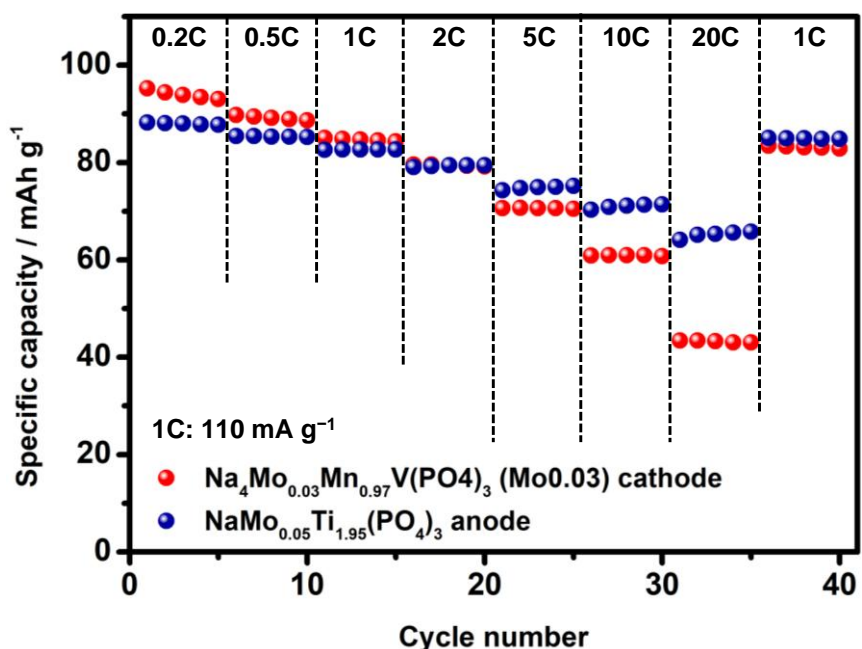


Figure S18. Rate performance of the $NaMo_{0.05}Ti_{1.95}(PO_4)_3$ anode and Mo0.03 cathode at several current densities.

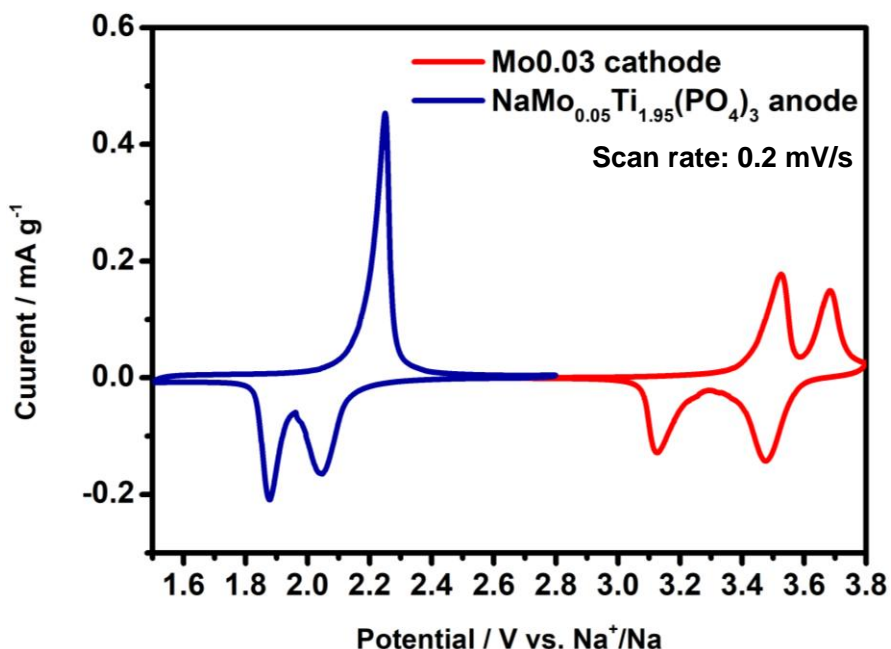


Figure S19. CV data of the $\text{NaMo}_{0.05}\text{Ti}_{1.95}(\text{PO}_4)_3$ anode and Mo0.03 cathode at a scan rate of 0.2 mV/s

References

- [1] X. Gao, R. Lian, L. He, Q. Fu, S. Indris, B. Schwarz, X. Wang, G. Chen, H. Ehrenberg, Y. Wei, Journal of Materials Chemistry A, 8 (2020) 17477-17486.
- [2] S. Ghosh, N. Barman, P. Senguttuvan, Small, 16 (2020) 2003973.
- [3] Z. Wang, G. Cui, Q. Zheng, X. Ren, Q. Yang, S. Yuan, X. Bao, C. Shu, Y. Zhang, L. Li, Small, (2023) 2206987.
- [4] V. Soundharajan, M.H. Alfaruqi, S. Lee, B. Sambandam, S. Kim, S. Kim, V. Mathew, D.T. Pham, J.-Y. Hwang, Y.-K. Sun, Journal of Materials Chemistry A, 8 (2020) 12055-12068.